



Contents lists available at ScienceDirect

Chinese Chemical Letters

journal homepage: [www.elsevier.com/locate/ccl](http://www.elsevier.com/locate/ccl)

Communication

# Ultralong nanowires self-assembled from a [b]-bisphenanthrene-fused azadipyrromethene

Wanle Sheng<sup>a</sup>, Zhangcui Wang<sup>a</sup>, Erhong Hao<sup>b,\*</sup>, Lijuan Jiao<sup>b,\*</sup><sup>a</sup> Department of Chemistry, Bengbu Medical College, Bengbu 233030, China<sup>b</sup> The Key Laboratory of Functional Molecular Solids, Ministry of Education, School of Chemistry and Materials Science, Anhui Normal University, Wuhu 241002, China

## ARTICLE INFO

## Article history:

Received 5 July 2020

Received in revised form 7 August 2020

Accepted 26 August 2020

Available online 27 August 2020

## Keywords:

AzaBODIPY  
Self-assembly  
H-aggregation  
Nanowire  
 $\pi$ -Extended

## ABSTRACT

The 1D microwires based on  $\pi$ -extended azaBODIPY were successfully prepared and characterized for the first time. The bisphenanthrene-fused **azaBPP-12C** with four hydrophobic chains was prepared through *de novo* synthesis method involving the Suzuki reaction and subsequent oxidative ring-fused coupling. The microwires and aggregation behavior were studied using SEM, XRD and absorption spectroscopy. Finally, an H-type aggregation was confirmed in the solution process.

© 2020 Chinese Chemical Society and Institute of Materia Medica, Chinese Academy of Medical Sciences. Published by Elsevier B.V. All rights reserved.

Organic compounds with polycyclic aromatic hydrocarbons generally show superior optoelectronic and self-assembling properties due to the  $\pi$ - $\pi$  interaction between molecules [1–3]. The self-assembly process is depending on molecular structure, which could be manipulated through molecular structure engineering [4–6]. This has been well demonstrated by the extensively studied hexabenzocoronene (HBC, Fig. 1) and their heteroatom-doped derivatives system, such as forming one dimensional (1D) micro- or nanowires [7,8], nanotubes [9–11], two dimensional (2D) nanosheets [12,13], which show great potential in electronic devices, such as organic field effect transistors and photodetectors [14,15].

Boron dipyrromethene dyes (BODIPYs) and their derivatives, as an increasingly valuable class of fluorophores, have been developed through various modification approaches [16–20]. Replacing the *meso* carbon atom of BODIPY by nitrogen atom to form azaBODIPY dyes (Fig. 1), which were first reported by O'Shea et al. have received extensive research interests lately due to their excellent stabilities (associated with their rigid structures) and their remarkable optic and electronic properties, especially the tunable deep-red to NIR absorptions/emissions [21–24]. Indeed,

their highly electron-deficient conjugation core skeletons with large dipole moments are ideal features for the promising organic electronics and self-assembly properties [25–27]. For example, the amphiphilic azaBODIPY molecule can self-assemble into globular nanoparticles and elongated nanorods by J-type aggregation mode [28–30]. The azaBODIPY molecule introduced with phosphoric acid can self-assemble to form nanosphere shells [31]. However, due to the limitation of the synthesis, there are few reports about the  $\pi$ -extended conjugated azaBODIPY. Until recently, we reported [a]- and [b]-bisphenanthrene-fused azaBODIPYs (azaBPP, Fig. 1) through oxidative aromatic coupling and palladium catalyst C–H activation reaction [32–35]. These  $\pi$ -extended azaBODIPY molecules not only exhibit excellent near infrared optical activity and interesting electronics properties, but also provide an opportunity to produce discrete (isolable) nanostructures through self-assembly. Despite the effects toward controlling and tuning the morphology of related porphyrinoids [36–38] and the above HBC molecules, the facile synthesis of well-defined, large nanostructures with NIR absorption over 800 nm, which have promising applications in important areas such as sensors, phototheranostic agents, and solar power, is still limited.

Herein, we synthesized a [b]-bisphenanthrene-fused azaBODIPY containing four long hydrophobic chains on the periphery (**azaBPP-12C**). Combined the  $\pi$ - $\pi$  and side chain interactions, **azaBPP-12C** can be self-assembled into one-dimensional microwires through the solution process. The microwires were

\* Corresponding authors.

E-mail addresses: [haohong@ahnu.edu.cn](mailto:haohong@ahnu.edu.cn) (E. Hao), [jiao421@ahnu.edu.cn](mailto:jiao421@ahnu.edu.cn) (L. Jiao).

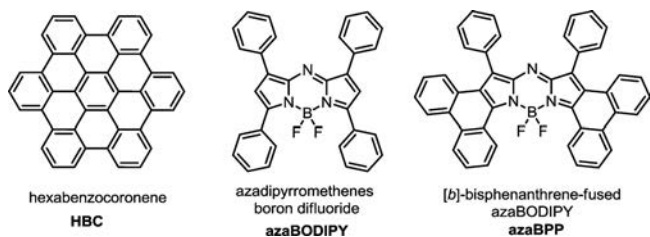


**Fig. 1.** Core structures of hexabenzocoronene (HBC), azadipyrromethenes boron difluoride (azaBODIPY) and [b]-bisphenanthrene-fused azaBODIPYs (azaBPP).

characterized using scanning electron microscope (SEM) and X-ray diffraction (XRD), the length can reach hundreds of microns. The aggregation behavior of **azaBPP-12C** in solution was confirmed as H-type aggregation by absorption spectroscopy.

[b]-PhenanthroazaBODIPY **azaBPP-12C** with four side chain was synthesized in Scheme 1. 1,3,5,7-Tetra-(4-dodecyloxyphenyl) azaBODIPY **3**, as the key starting material with long chain installed initially, was generated in an overall yield of 30% in three steps (Scheme S1 in Supporting information) from commercially available 4-dodecyloxybenzaldehyde and 4-dodecyloxyacetophenone. After bromination, the dibromoazaBODIPY **2** was then applied in the Suzuki coupling reaction with 4-*tert*-butylphenylboronic acid to afford the corresponding azaBODIPY **1** in 77% yield (Scheme 1). The subsequent oxidative ring-fusion reaction with 10 equiv. of  $\text{FeCl}_3$  in  $\text{CH}_2\text{Cl}_2/\text{CH}_3\text{NO}_2$  at room temperature afforded target product **azaBPP-12C** successfully in high yield.

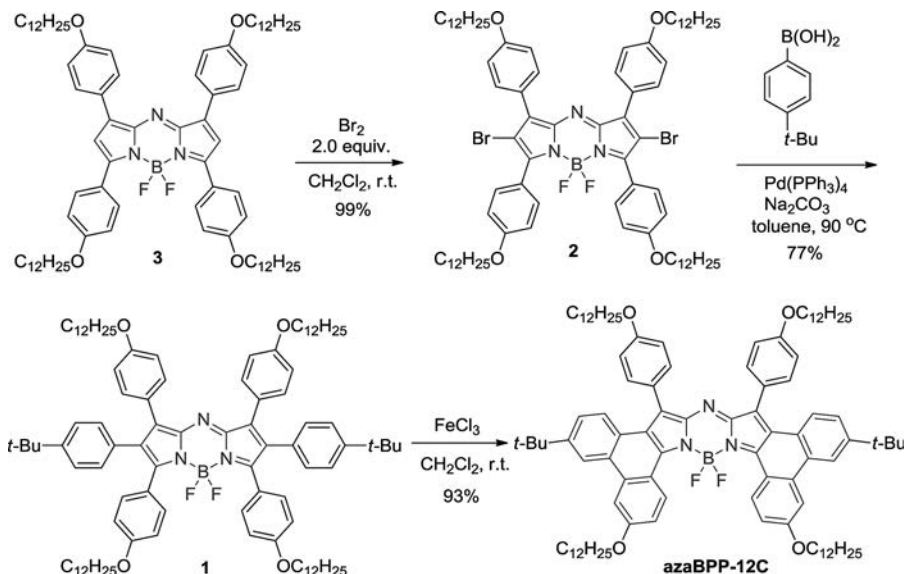
The UV–vis absorption as well as fluorescence spectra of **1** and **azaBPP-12C** in chloroform (Fig. 2) show all of the typical spectral features of substituted azaBODIPY and [b]-phenanthroazaBODIPYs reported in the literatures [33,34]. Compound **1** exhibits absorption band around 580–730 nm, with a maximum peak at 657 nm and the corresponding emission maximum at 683 nm ( $\phi = 0.25$ ). After the cyclization, the absorption bands of **azaBPP-12C** undergo significant red shifts to 700–830 nm, with the maximum absorption peak at 790 nm. The molar extinction coefficient value of the ring-fusion compounds **azaBPP-12C** reaches

$173,800 \text{ L mol}^{-1} \text{ cm}^{-1}$ , which is double greater than that of **1** ( $74,100 \text{ L mol}^{-1} \text{ cm}^{-1}$ ).

The self-assembly behaviors of **azaBPP-12C** in solution was monitored by the absorption spectral measurement. Initially, **azaBPP-12C** keeps the original characteristic absorption peak in THF (Fig. 3a). Progressively increasing the volume fraction of water, as a poor solvent, in THF does not affect its spectrum until the solution consists of 70% water. The intensity of the main absorption band was decreased greatly, while the absorption at shorter wavelength became enhanced. No red-shifted absorption band was observed, which indicated that an H-aggregation of **azaBPP-12C** was formed during the aggregation process [39,40]. Continuing to increase the fraction of water to 90%, the absorption intensity of the short wavelength was increased with a slight lift up around 850 nm, which may be due to the extended aggregate states. The same aggregation process was also detected in ethanol solution (Fig. 3b). As time goes on, the absorption below 790 nm was gradually decreased, while the absorption at shorter wavelength became enhanced. These results indicate the dominant role of  $\pi$ - $\pi$  interaction between the molecules of **azaBPP-12C**.

The face-to-face arrangement of  $\pi$ - $\pi$  interaction between the molecules typically guarantees the formation of 1D materials [41]. The morphology of the aggregates formed was then examined by scanning electron microscopy (SEM). Initially, we used the method of poor solvent mixing to prepare the aggregates. At room temperature, methanol continuously mixed into the chloroform solution of **azaBPP-12C**. As the poor solvent methanol continuously increased, the solubility of the mixed solvent to **azaBPP-12C** was decreased. Under  $\pi$ - $\pi$  intermolecular interaction and alkyl chain interaction, one-dimensional nanowires were indeed gradually formed (Fig. S1 in Supporting information). However, the speed of poor solvent mixing may be too fast, the nanowires formed by this method have great defects.

Finally, the well-ordered 1D nanowires of **azaBPP-12C** were precipitated by cooling hot saturated solution. A suspension of **azaBPP-12C** in MeOH/THF (ratio: 1/2) was heated to form a homogeneous solution. Then the solution was cooled to room temperature slowly, allowing the molecules to self-assemble. The nanowires obtained in MeOH/THF mixed solvent are around  $1 \mu\text{m}$  in width and hundreds of micrometers in length (Figs. 4a-b and



**Scheme 1.** Synthesis of [b]-Bisphenanthrene-Fused AzaBODIPYs **azaBPP-12C**.

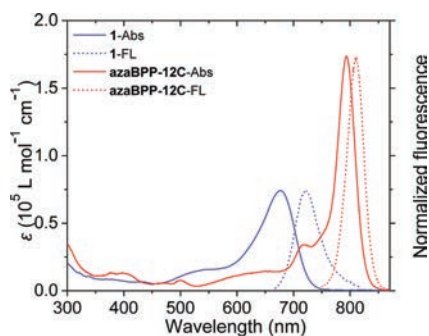


Fig. 2. Absorption (Abs) and fluorescence (FL) spectra of compounds **1** and **azaBPP-12C** in chloroform ( $5 \times 10^{-6}$  mol/L).

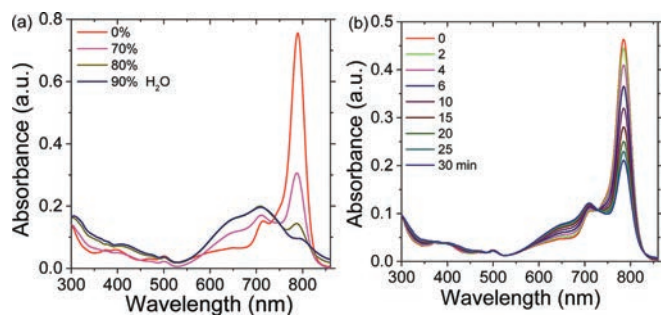


Fig. 3. Spectroscopic changes observed during aggregation for **azaBPP-12C**: (a) Evolution of the absorption spectrum as the water content increased from 0 to 90% (v/v) in THF/water mixture ( $4 \times 10^{-6}$  mol/L). (b) Evolution of the absorption spectrum in ethanol at different aging times: from 0 to 30 min ( $3 \times 10^{-6}$  mol/L).

Fig. S2 in Supporting information). The microwires were further characterized by the X-ray diffraction analysis. The first and second diffraction peaks ( $d$ -spacing = 21.8 and 17.0 Å) are assigned to the edge-to-edge distances between adjacent **azaBPP-12C** molecules at the long and short axis directions (Fig. 4g). The broad diffuse scattering was observed in the middle-angle region ( $d$ -spacing = 7.1 Å), which is characteristic of the liquid-like order of the hydrocarbon chains. Combined with absorption spectral results, these data indicated that the molecules adopt face to face arrangement. A one-dimensional columnar arrangement model was proposed (Fig. 4h). The diffraction peaks in the high-angle region ( $d$ -spacing = 4.3 and 4.4 Å) were assigned to the periodic correlations of the cores along the columns.

When the solvent is changed from MeOH/THF mixed solvent to *n*-hexane or 1,4-dioxane, respectively, similar nanowires were also observed in both solvents using the same method (Figs. 4c–f). However, the nanowires obtained in hexane are much thinner, with a width around 500 nm, while the nanowires obtained in 1,4-dioxane are thicker and more rigid, with a width around 2 μm. In addition, these nanowires obtained in both 1,4-dioxane and *n*-hexane look softer compared to those obtained in MeOH/THF mixed solvent. These changes in the morphology of self-assembled nanoscale aggregates indicated the solvent effect on the formation of self-assembled nanostructures of **azaBPP-12C** molecules.

In summary, a [*b*]-bisphenanthrene-fused azaBODIPY with four side chain was prepared through the de novo synthesis method. This  $\pi$ -extended azaBODIPY shows strong, red-shifted absorption and emission in NIR region with maximum peaks up to 793 nm and 810 nm, respectively. Due to the enhanced  $\pi$ - $\pi$  interaction, **azaBPP-12C** adopted H-aggregation during the aggregation. The ordered 1D microwires are also obtained by solution process and characterized using SEM and XRD, which are promising materials for the application in organic devices.

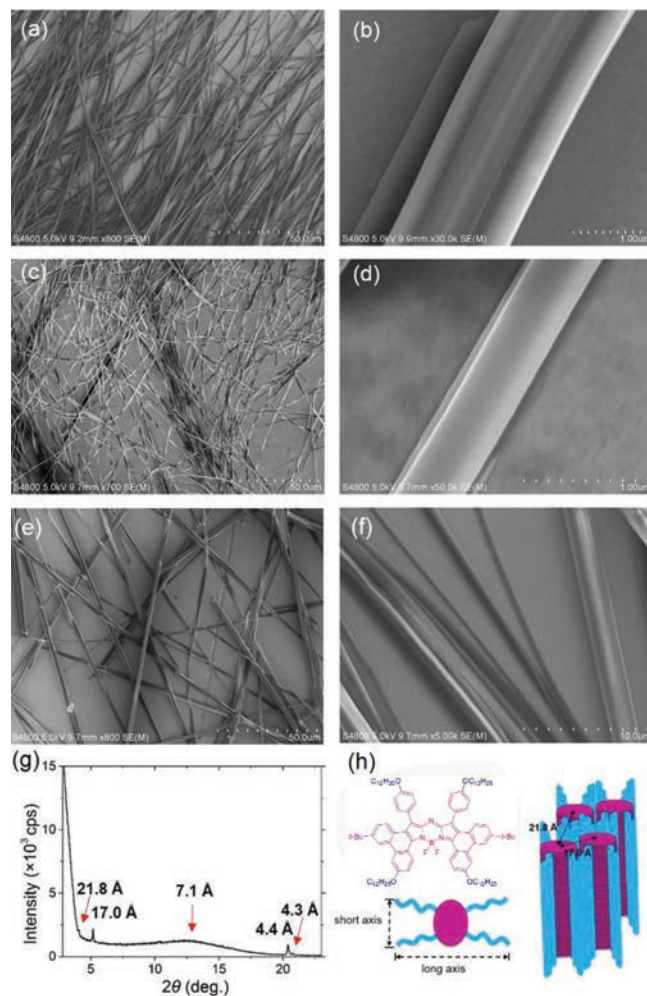


Fig. 4. (a, b) SEM images (a, scale bar: 50 μm; b, scale bar: 1 μm) and (g) XRD pattern of the nanowires grown from 1:2 MeOH:THF solvent. (c, d) SEM images of the nanowires grown from *n*-hexane (scale bar: c, 50 μm; d, 1 μm). (e, f) SEM images of the nanowires grown from 1,4-dioxane (scale bar: e, 50 μm; f, 10 μm). (h) The proposed model of the columnar stacking structure for **azaBPP-12C**.

#### Declaration of competing interest

The authors declare that they have no known competing financial interests or personal relationships that could have appeared to influence the work reported in this paper.

#### Acknowledgments

This work is supported by the National Nature Science Foundation of China (Nos. 21672006, 21672007, 21871006), Laboratorial Open Fund of Ministry of Education of Anhui Normal University (No. FMS201914), and Natural Science Research Fund of BengBu Medical College (No. BYKY2019005ZD).

#### Appendix A. Supplementary data

Supplementary material related to this article can be found, in the online version, at doi:<https://doi.org/10.1016/j.ccllet.2020.08.047>.

#### References

- [1] M. Stępień, E. Gońka, M. Żyłaa, N. Sprutta, Chem. Rev. 117 (2017) 3479–3716.
- [2] X. Luo, J. Li, J. Zhao, et al., Chin. Chem. Lett. 30 (2019) 839–846.
- [3] Q. Fan, W. Ni, L. Chen, G.G. Gurzadyan, Y. Xiao, Chin. Chem. Lett. 31 (2020) 2965–2969.

- [4] X. Zhang, Q. Wang, L. Wu, et al., *J. Phys. Chem. B* 114 (2010) 1233–1240.
- [5] M. Al Kobaisi, S.V. Bhosale, K. Latham, A.M. Raynor, S.V. Bhosale, *Chem. Rev.* 116 (2016) 11685–11796.
- [6] Z. Li, S. Chen, C. Gao, et al., *J. Am. Chem. Soc.* 141 (2019) 19448–19457.
- [7] M. Kastler, W. Pisula, D. Wasserfallen, T. Pakula, K. Müllen, *J. Am. Chem. Soc.* 127 (2005) 4286–4296.
- [8] X.Y. Wang, F.D. Zhuang, R.B. Wang, et al., *J. Am. Chem. Soc.* 136 (2014) 3764–3767.
- [9] W. Jin, Y. Yamamoto, T. Fukushima, et al., *J. Am. Chem. Soc.* 130 (2008) 9434–9440.
- [10] W. Zhang, W. Jin, T. Fukushima, N. Ishii, T. Aida, *J. Am. Chem. Soc.* 135 (2013) 114–117.
- [11] Y. Liu, W. Zeng, X. Li, W. Jin, D. Zhang, *Dye. Pigment.* 163 (2019) 553–558.
- [12] J. Luo, X. Xu, R. Miao, Q. Miao, *J. Am. Chem. Soc.* 134 (2012) 13796–13803.
- [13] Y. Zhou, M.Y. Zhang, K.H. Gu, et al., *Asian J. Org. Chem.* 4 (2015) 746–755.
- [14] T. Aida, E.W. Meijer, S.I. Stupp, *Science* 335 (2012) 813–817.
- [15] T. Shimizu, W. Ding, N. Kameta, *Chem. Rev.* 120 (2020) 2347–2407.
- [16] Q. Wang, X. Wei, C. Li, Y. Xie, *Dye. Pigment.* 148 (2018) 212–218.
- [17] F. Ma, L. Zhou, Q. Liu, C. Li, Y. Xie, *Org. Lett.* 21 (2019) 733–736.
- [18] G. Su, K. Zhang, F. Sha, et al., *Dye. Pigment.* 180 (2020) 108504.
- [19] W. Sheng, F. Lv, B. Tang, E. Hao, L. Jiao, *Chin. Chem. Lett.* 30 (2019) 1825–1833.
- [20] D. Wang, X. Guo, H. Wu, et al., *J. Org. Chem.* 85 (2020) 8360–8370.
- [21] Y. Ge, D.F. O’Shea, *Chem. Soc. Rev.* 45 (2016) 3846–3864.
- [22] K. Burgess, A. Loudet, *Chem. Rev.* 107 (2007) 4891–4832.
- [23] H. Lu, J. Mack, Y. Yang, Z. Shen, *Chem. Soc. Rev.* 43 (2014) 4778–4823.
- [24] Z. Wang, C. Cheng, Z. Kang, et al., *J. Org. Chem.* 84 (2019) 2732–2740.
- [25] H. Wang, Y. Zhang, Y. Chen, et al., *Angew. Chem. Int. Ed.* 59 (2020) 5185–5192.
- [26] Y. Liu, N. Song, Z. Li, L. Chen, Z. Xie, *Dye. Pigment.* 160 (2019) 71–78.
- [27] C. Liu, W. Ding, Y. Liu, H. Zhao, X. Cheng, *New J. Chem.* 44 (2020) 102–109.
- [28] Z. Chen, Y. Liu, W. Wagner, et al., *Angew. Chem. Int. Ed.* 56 (2017) 5729–5733.
- [29] Y. liu, Y. Zhang, F. Fennel, et al., *Chem. Eur. J.* 24 (2018) 16388–16394.
- [30] Y. Chen, X.H. Zhang, D.B. Cheng, et al., *ACS Nano* 14 (2020) 3640–3650.
- [31] M.H.Y. Cheng, K.M. Harmatys, D.M. Charron, J. Chen, G. Zheng, *Angew. Chem. Int. Ed.* 58 (2019) 13394–13399.
- [32] J. Cui, W. Sheng, Q. Wu, et al., *Chem. Asian J.* 12 (2017) 2486–2493.
- [33] W. Sheng, J. Cui, Z. Ruan, et al., *J. Org. Chem.* 82 (2017) 10341–10349.
- [34] W. Sheng, Y.Q. Zheng, Q. Wu, et al., *Org. Lett.* 19 (2017) 2893–2896.
- [35] W. Sheng, Y. Wu, C. Yu, et al., *Org. Lett.* 20 (2018) 2620–2623.
- [36] Y. Gao, X. Zhang, C. Ma, X. Li, J. Jiang, *J. Am. Chem. Soc.* 130 (2008) 17044–17052.
- [37] Y. Gao, Y. Chen, R. Li, et al., *Chem. Eur. J.* 15 (2009) 13241–13252.
- [38] P. Guo, P. Chen, M. Liu, *Langmuir* 28 (2012) 15482–15490.
- [39] F. Würthner, T.E. Kaiser, C.R. Saha-Möller, *Angew. Chem. Int. Ed.* 50 (2011) 3376–3410.
- [40] T. Li, J. Benduhn, Z. Qia, et al., *J. Phys. Chem. Lett.* 10 (2019) 2684–2691.
- [41] Y. Guo, L. Xu, H. Liu, et al., *Adv. Mater.* 27 (2015) 985–1013.